A&A 449, 855–859 (2006)
DOI: 10.1051/0004-6361:20054136

Astronomy & Astrophysics

Linelists for NH_3, NH_2D, ND_2H, and ND_3 with quadrupole coupling hyperfine components⋆

L. H. Coudert[1] and E. Roueff[2]

[1] LISA, UMR 7583 du CNRS, Université Paris 12, 61 Avenue du Général de Gaulle, 94010 Creteil Cedex, France
e-mail: coudert@lisa.univ-paris12.fr
[2] LUTH and UMR 8102 du CNRS, Observatoire de Paris, Section de Meudon, 5 Place J. Janssen, 92195 Meudon, France
e-mail: evelyne.roueff@obspm.fr

Received 31 August 2005 / Accepted 17 November 2005

ABSTRACT

Linelists for the ammonia molecule and its three deuterated variants NH_2D, ND_2H, and ND_3 are built taking hyperfine quadrupole coupling effects into account. For each hyperfine component, the line frequency, the line intensity, and the lower level energy are calculated.

Key words. molecular data – catalogs – radio lines: ISM

1. Introduction

The molecular hyperfine structure of microwave transitions is a powerful way to identify the presence of saturation effects in an astronomical spectrum. Indeed, the intensity ratios of various hyperfine components is well known, as it is tabulated in basic molecular spectroscopy books (Townes & Schawlow 1955), and it provides an efficient test of optically thin transitions. However, this knowledge is available only for a restricted number of molecules, amongst which nitrogen molecules such as CN, N_2H^+, HCN play an important role. The recent astrophysical detection of NH_2D (Tiné et al. 2000), ND_2H (Roueff et al. 2000; Lis et al. 2005, 2006), and ND_3 (Lis et al. 2002; van der Tak et al. 2002; Roueff et al. 2005) at an unprecedented level has prompted us to consider the various deuterated isotopologs of ammonia.

Nitrogen-containing molecules display a strong quadrupole coupling arising from the nitrogen atom and leading to splittings of the microwave lines on the order of 2 MHz (Kukolich & Wofsy 1970). The observation of such splittings is straightforward considering the present capabilities of radio astronomical techniques, and the individual hyperfine components may indeed be resolved in cold dense clouds and pre-stellar clouds such as L 134N, L 1544, L 1689, and B 1 (Pagani et al. 2003, 2004, 2005; Lis et al. 2006) where linewidths on the order of 0.3 $\mathrm{km\,s^{-1}}$ are found. It is also valuable to account for the different hyperfine components of a particular transition in a region with larger turbulent velocities so as to reconstruct the whole profile. This also justifies calculation of the quadrupole coupling hyperfine structure of nitrogen-containing molecules and of the deuterated isotopologs of ammonia.

The present paper is concerned with a calculation of the rotational spectra of ammonia and its three deuterated isotopologs, accounting for the hyperfine coupling effects. The molecules being considered are the ammonia molecule NH_3 and its deuterated variants NH_2D, ND_2H, and ND_3. These four species can either be found in the CDMS (Müller et al. 2001) or in the JPL (Pickett et al. 1998) data bases. However, except for NH_2D and ND_3 and only for low J-values for the latter molecule, the spectroscopic data available do not include information on hyperfine effects.

2. Spectroscopic calculation

2.1. Rovibrational wavefunctions, line frequencies, and line intensities

The four molecules dealt with display an inversion large-amplitude motion leading to a tunneling splitting of their vibrational states. The lower and upper tunneling sublevels arising from the ground vibrational state are labeled 0s and 0a, respectively.

For the two symmetrical species NH_3 and ND_3, the molecule-fixed xyz-axis system is attached to the molecule so that the z-axis is parallel to the c-axis, which is the 3-fold symmetry axis. For the two asymmetrical species, the y-axis is parallel to the b-axis in the case of NH_2D and to the a-axis in the case of ND_2H. The x- and z-axes are attached to the molecule,

⋆ Tables 8–11 are only available in electronic form at the CDS via anonymous ftp to cdsarc.u-strasbg.fr (130.79.128.5) or via http://cdsweb.u-strasbg.fr/cgi-bin/qcat?J/A+A/449/855

making the same choice as Cohen & Pickett (1982). The angle between the c- and z-axes is a few degrees.

For the symmetrical as for the asymmetrical species, coupling between the overall rotation and the inversion large amplitude motion leads to a mixing of the 0s and 0a tunneling sublevels. For a rotational-tunneling level n, characterized by a total value J of the rotational angular momentum, the rotational-tunneling wavefunction Ψ^n_{rt} assumes the following expression

$$|\Psi^n_{rt}\rangle = \sum_{k,\alpha} a^n_s(J,k,\alpha)|J,k,\alpha\rangle|0s\rangle + \sum_{k,\alpha} a^n_a(J,k,\alpha)|J,k,\alpha\rangle|0a\rangle \quad (1)$$

where $a^n_s(J,k,\alpha)$ and $a^n_a(J,k,\alpha)$ are numerical coefficients, and where $|J,k,\alpha\rangle$, with $0 \le k \le J$ and $\alpha = \pm 1$, are Wang-type linear combinations of symmetric top-rotational functions. For $k > 0$, $|J,k,\alpha\rangle = [|J,k\rangle + \alpha|J,-k\rangle]/\sqrt{2}$; for $k = 0$, $|J,k,\alpha\rangle = |J,0\rangle$. In the case of the symmetrical species NH_3 and ND_3, the tunneling sublevel mixing arises because of a distortion term in the effective rovibrational Hamiltonian (Fusina et al. 1985). In the case of the asymmetrical species NH_2D and ND_2H, this mixing is due to a zeroth-order term in the rovibrational Hamiltonian (Cohen & Pickett 1982).

For all four species, energy levels were computed in order to obtain partition functions as well as transition frequencies. These calculations are based on fits to already available data. For NH_3, the partition function was evaluated by refitting the far-infrared data of Poynter & Margolis (1983) and setting the constants ${}^{(s)}D_K$, ${}^{(s)}H_K$, ${}^{(s)}L_K$, η^{JJ}_3, η_6, and α^0 to the values published by Urban et al. (1983). Calculation of the rotational spectrum is based on a fit of a more accurate data set involving the far-infrared data of Poynter & Margolis (1983) and the microwave data of Poynter & Kakar (1975) and Helminger et al. (1971). For the other isotopic species, the same calculation was used for evaluating the partition function and for predicting the rotational spectrum. For ND_3, the microwave data reported by Helminger & Gordy (1969), Helminger et al. (1971), and Fusina & Murzin (1994) were refitted, along with the far-infrared data of Fusina et al. (1985). For NH_2D and ND_2H, the spectroscopic data measured by De Lucia & Helminger (1975), Cohen & Pickett (1982), and Fusina et al. (1988) were reanalyzed. For all four species, rotational-tunneling energies and wavefunctions, that is, the coefficients appearing in Eq. (1), were obtained for both tunneling sublevels.

Line strengths were calculated assuming constant values for the dipole moment matrix elements. For NH_3 and ND_3, only one matrix element is needed: $\mu^{sa}_z = \langle 0s|\mu_z|0a\rangle$. Its value was taken from Marshall & Muenter (1981) and Di Lonardo & Trombetti (1981) for NH_3 and ND_3, respectively. For the asymmetrical species NH_2D and ND_2H, the matrix elements $\mu^{ss}_x = \langle 0s|\mu_x|0s\rangle$ and $\mu^{aa}_x = \langle 0a|\mu_x|0a\rangle$ are also required (Job et al. 1987). For these two species these matrix elements were taken from Cohen & Pickett (1982). Table 1 gives the values used for all dipole moment matrix elements.

Partition functions were computed for several temperatures. The degeneracy factors used account for the equivalent hydrogen or deuterium atoms and include the $(2J + 1)$ factor. Table 2 gives the values obtained for the partition functions. For all four species, a zero value was taken for the energy of the 0s levels when $J = 0$. Contributions from the 1a and 1s states were included. For the symmetrical species NH_3 and ND_3, rotational levels, their symmetry species, and the statistical weight used in the calculation are listed up to $J = 2$ in Table 3. For the asymmetrical species NH_2D and ND_2H, the same quantities are listed in Table 4. In both tables, statistical weights are also given including the two contributions mentioned above.

Table 1. Numerical values, in Debye, used for the dipole moment components matrix elements in the line-intensity calculation.

	NH_3	NH_2D	ND_2H	ND_3
μ^{as}_z	1.471	1.465	1.482	1.497
$\mu^{ss}_x = \mu^{aa}_x$	0.0	−0.184	0.211	0.0

Table 2. Numerical values for the partition functions listed for several values of the temperature T in Kelvin.

T/K	NH_3	NH_2D	ND_2H	ND_3
9.375	5.079	8.488	8.653	35.285
18.750	10.914	21.638	22.355	89.427
37.500	27.192	58.190	60.523	242.556
75.000	74.004	160.547	167.583	673.209
150.000	206.352	448.987	469.586	1888.115
225.000	378.533	825.129	864.978	3485.304
300.000	587.191	1283.341	1350.478	5462.490

Table 3. For NH_3 and ND_3, rotational-tunneling quantum numbers, symmetry species in D_{3h}, energy values in cm^{-1}, and statistical weights up to $J = 2$.

				NH_3		ND_3	
J	K	v	Γ	E	g	E	g
0	0	0s	A'_1	0.0	0	0.0	10
1	0	0s	A'_2	19.8899	12	10.2847	3
1	1	0s	E''	16.1723	6	8.2672	24
2	0	0s	A'_1	59.6493	0	30.8494	50
2	1	0s	E''	55.9381	10	28.8333	40
2	2	0s	E'	44.7945	10	22.7851	40
0	0	0a	A''_2	0.7934	4	0.0531	1
1	0	0a	A''_1	20.6733	0	10.3375	30
1	1	0a	E'	16.9627	6	8.3202	24
2	0	0a	A''_2	60.4130	20	30.9015	5
2	1	0a	E'	56.7086	10	28.8857	40
2	2	0a	E''	45.5858	10	22.8382	40

2.2. Hyperfine-coupling Hamiltonian and energies

The quadrupole coupling Hamiltonian W used here is the equivalent operator arising when only $\Delta J = 0$ matrix elements are sought (Hougen & Oka 1981; Aliev & Hougen 1984):

$$W = eQ\left[\sum_{\alpha\beta} q_{\alpha\beta}\, J_\alpha J_\beta\right] F(I,J) \quad (2)$$

Table 4. For NH_2D and ND_2H, rotational-tunneling quantum numbers, energy values in cm^{-1}, symmetry species in C_{2v}, and statistical weights up to $J = 2$.

		NH_2D			ND_2H		
J_{K_a,K_c}	v	E	Γ	g	E	Γ	g
0_{00}	0s	0.0	A_1	1	0.0	A_1	2
1_{01}	0s	11.1018	A_2	3	9.0971	B_1	3
1_{11}	0s	14.3725	B_1	9	11.1915	A_2	6
1_{10}	0s	16.0925	B_2	9	12.7962	B_2	3
2_{02}	0s	32.7820	A_1	5	26.6565	A_1	10
2_{12}	0s	34.8518	B_2	15	27.7797	B_2	5
2_{11}	0s	40.0099	B_1	15	32.5913	A_2	10
2_{21}	0s	49.8154	A_2	5	38.8689	B_1	5
2_{20}	0s	50.3348	A_1	5	39.5018	A_1	10
0_{00}	0a	0.4059	B_1	3	0.1707	B_1	1
1_{01}	0a	11.5063	B_2	9	9.2677	A_1	6
1_{11}	0a	14.7761	A_1	3	11.3600	B_2	3
1_{10}	0a	16.4932	A_2	3	12.9640	A_2	6
2_{02}	0a	33.1852	B_1	15	26.8270	B_1	5
2_{12}	0a	35.2555	A_2	5	27.9487	A_2	10
2_{11}	0a	40.4051	A_1	5	32.7584	B_2	5
2_{21}	0a	50.2077	B_2	15	39.0294	A_1	10
2_{20}	0a	50.7258	B_1	15	39.6623	B_1	5

where α and β run over the molecule-fixed coordinates x, y, z, the symbol e denotes the electronic charge, Q is the nuclear quadrupole moment, $q_{\alpha\beta}$ is the electric field gradient tensor, J_α are components of the rotational angular momentum $\boldsymbol{J}$, and

$$F(I,J) = \frac{\left[3(\boldsymbol{I}\cdot\boldsymbol{J})^2 + \frac{3}{2}\boldsymbol{I}\cdot\boldsymbol{J} - \boldsymbol{I}^2\boldsymbol{J}^2\right]}{[I(2I-1)J(J+1)(2J-1)(2J+3)]}, \quad (3)$$

$\boldsymbol{I}$ being the nuclear spin operator and I the corresponding quantum number. Taking the coupling scheme $\boldsymbol{F} = \boldsymbol{I} + \boldsymbol{J}$, where $\boldsymbol{F}$ is the total angular momentum characterized by the quantum number F such that $|J - I| \le F \le J + I$, Eq. (2) allows us to obtain a closed-form expression of the hyperfine energy $E(F, n)$ of the rotational-tunneling level n

$$E(F,n) = \frac{(eQq_J)_n}{2I(2I-1)J(2J-1)}\left[\frac{3}{4}C(C+1) - I(I+1)J(J+1)\right] \quad (4)$$

where $C = F(F+1) - I(I+1) - J(J+1)$, and $(eQq_J)_n$ is a constant term depending only on the rotational-tunneling quantum numbers

$$(eQq_J)_n = \langle\Psi^n_{rt}| \sum_{\alpha\beta} eQq_{\alpha\beta} J_\alpha J_\beta |\Psi^n_{rt}\rangle \frac{2}{(J+1)(2J+3)}. \quad (5)$$

This matrix element is evaluated by assuming that the electric-field gradient tensor has the following matrix elements

$$\langle 0s|eQq_{\alpha\beta}|0s\rangle = \langle 0a|eQq_{\alpha\beta}|0a\rangle = \chi_{\alpha\beta} \quad \text{and}$$
$$\langle 0s|eQq_{\alpha\beta}|0a\rangle = 0 \quad (6)$$

where $\chi_{\alpha\beta}$ are the components of the zero-trace effective quadrupole coupling tensor. The values used to build the data bases are given in Table 5. For NH_3, they were obtained from Hougen (1972). For NH_2D these values were obtained by fitting the hyperfine splitting reported by Cohen & Pickett (1982). For ND_2H, they were obtained from the results reported by Garvey et al. (1976). At last, for ND_3, they come from the results of van Veldhoven et al. (2002).

Table 5. Numerical values in MHz for the diagonal components of the effective quadrupole coupling tensor. In the case of NH_3, the J- and K-dependence of these components was also taken into account (Hougen 1972).

$\chi_{\alpha\alpha}$	NH_3	NH_2D	ND_2H	ND_3
χ_{xx}	2.04482	1.903731	1.815002	2.041
χ_{yy}	2.04482	2.044097	2.045000	2.041
χ_{zz}	−4.08965	−3.947828	−3.860002	−4.083

Computing the hyperfine components intensities requires calculating their line strengths. For the hyperfine components between the $|n'J'F'\rangle$ and $|nJF\rangle$ levels, the line strength $S(n'J'F', nJF)$ is the square of the electric dipole moment matrix elements, summed over the degenerate magnetic states of the transition

$$S(n'J'F', nJF) = \sum_{M'_F, M_F, \gamma} \left|\langle n', J', F', M'_F|\, \mu_\gamma\, |n, J, F, M_F\rangle\right|^2 \quad (7)$$

where μ_γ with $\gamma = X, Y$, and Z are the components of the dipole moment in the laboratory-fixed axis system. In agreement with Thaddeus et al. (1964), the strength of the hyperfine component is expressed with $S(n'J', nJ)$ that of the rotational-tunneling transitions using

$$S(n'J'F', nJF) = (2F'+1)(2F+1)\left|\begin{Bmatrix} I & J' & F' \\ 1 & F & J \end{Bmatrix}\right|^2 S(n'J', nJ). \quad (8)$$

3. Generating the linelists

The linelists were built by calculating the frequencies of the allowed rotational-tunneling transitions characterized by a lower and an upper rotational quantum number J smaller than 8. It was not deemed necessary to consider a higher maximum J-value as the hyperfine splittings decrease with J, and the relative intensities of the hyperfine components become large (Townes & Schawlow 1955). For all allowed rotational-tunneling transitions, integrated intensities were calculated in nm^2 MHz units at 300 K using the results given in Tables 1 and 2. Just as in the JPL (Pickett et al. 1998) data bases, the selected transitions are those with an intensity in nm^2 MHz units at 300 K larger than

$$10^{\mathrm{LOGSTR0}} + (\nu/300\,000)^2 \times 10^{\mathrm{LOGSTR1}} \quad (9)$$

where ν is the frequency in MHz, and LOGSTR0 and LOGSTR1 are two constants. For all four species, Table 6 lists the values used for these two constants. For NH_3, rotational-tunneling transitions with $\Delta K > 0$ having a sufficient intensity with Eq. (9) were nonetheless excluded from the data base, as their frequencies could not be predicted with sufficient accuracy.

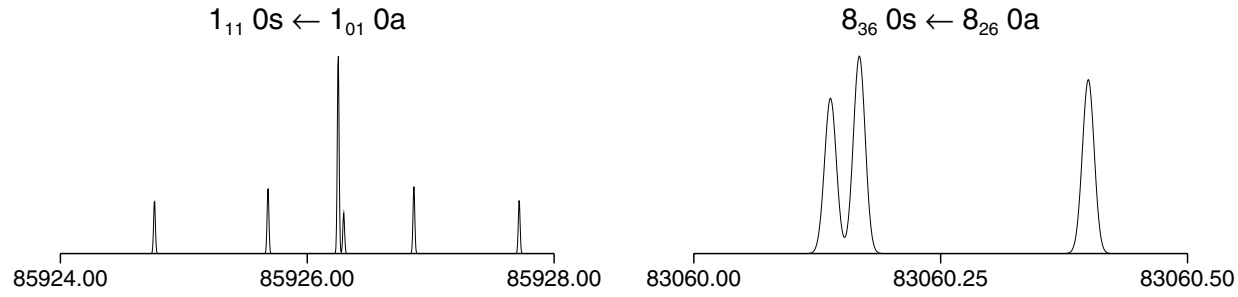

Fig. 1. For two Q-type transitions, calculated hyperfine patterns plotted for NH_2D. Numbers on the x-axis correspond to frequencies in MHz units. A Gaussian line-shape was assumed for the hyperfine components with a half width at half height of 0.010 MHz $\approx$ 0.035 km s^{-1}. Due to the different J-values, the pattern on the *left* (*right*) spans a frequency range of 4 MHz $\approx$ 14 km s^{-1} (0.5 MHz $\approx$ 1.8 km s^{-1}).

Table 6. Numerical values, for the parameters used to calculate the intensity cutoff in Eq. (9).

	NH_3	NH_2D	ND_2H	ND_3
LOGSTR0	−15.2	−9.5	−9.0	−9.3
LOGSTR1	−11.0	−7.0	−7.0	−6.3

In many cases, calculated frequencies were replaced for all four species by their observed values. For NH_3, all calculated frequencies were replaced by their observed values. For $\Delta J = 0$ transitions and the $J = 1 \leftarrow 0$ transition, for which there are accurate microwave data, this leads to smaller changes than 12 kHz. For the higher frequency $J+1 \leftarrow J$ transitions with $J \geq 1$, for which observed frequencies can only be retrieved from the FIR wavenumbers reported by Poynter & Kakar (1975), this leads to changes as large as 22 MHz. Because the normal species of ammonia is a light molecule for which distortion effects are important, we believe that observed frequencies for these R-type transitions are more accurate than calculated ones. For NH_2D, ND_2H, and ND_3, calculated frequencies were replaced by their observed values, but only for those transitions for which accurate microwave frequencies are available. For these three species, this leads to frequency changes that are smaller than 1 MHz. For all four species, uncertainties in the calculated frequencies were retrieved from the analyses described in Sect. 2. When this calculated value was smaller than 10 kHz, the uncertainty was set to 10 kHz. For transitions for which the calculated frequency was replaced by the the observed one, the uncertainty quoted by the authors was used.

For the selected rotational-tunneling transitions, hyperfine components frequencies and intensities were then calculated using Eqs. (4) and (8) and Table 5. Figure 1 shows calculated hyperfine patterns for two Q-type transitions, as obtained from the linelist built for NH_2D. Hyperfine effects are greater for the transition characterized by a smaller J-value.

A comparison was carried out of the present linelists with those available in the CDMS (Müller et al. 2001) data base for NH_2D, ND_2H, and ND_3 and in the JPL (Pickett et al. 1998) data base for NH_3. For NH_2D and ND_3, for which hyperfine effects are taken into account in the CDMS (Müller et al. 2001) data base, the frequency and intensity of hyperfine components were compared. For the other two species, the frequency and the intensity of rotational-tunneling transitions were compared. Table 7 summarizes the results for the comparison of the frequencies. In this table, the highest values of the difference for each species between the frequency calculated in this work and those calculated in either the CDMS (Müller et al. 2001) or the JPL (Pickett et al. 1998) data bases are given. Positive and negative difference values appear, and the root mean square deviation of this difference is also given. The discrepancies between the present linelists and those available from the CDMS (Müller et al. 2001) or the JPL (Pickett et al. 1998) data bases stem from the fact that the frequency calculations are based on analyses of different data sets. For the intensities, the comparison shows that the line intensities calculated in the present work are within 5% from those of either the CDMS (Müller et al. 2001) or the JPL (Pickett et al. 1998) data bases.

Table 7. For each species, the largest values, in MHz, of the difference between the frequencies calculated in this work and those available from either the CDMS (Müller et al. 2001) or the JPL (Pickett et al. 1998) data bases. The column headed "Positive difference" ("Negative difference") gives the largest differences with a positive (negative) value. The column headed "rms" gives the root mean square deviation of this difference.

Species	Positive difference	Negative difference	rms
NH_3	0.12	−0.15	0.07
NH_2D	1.19	−2.31	0.52
ND_2H	8.10	−10.89	1.91
ND_3	0.11	−0.51	0.19

For NH_3, NH_2D, ND_2H, and ND_3, the linelists are given respectively in Tables 8–11, which are available at the CDS. Each table is formatted as the catalog line file of the JPL (Pickett et al. 1998) data base, so they have 10 columns. The first, second, and third columns contain the line frequency in MHz, the error in MHz, and the base 10 logarithm of the line intensity in nm^2 MHz at 300 K. The fourth, fifth, and sixth columns give the degrees of freedom of the rotational partition function, the lower state energy in cm^{-1}, and the upper state degeneracy, respectively. The seventh and eighth columns contain tag numbers. At last, the ninth and tenth columns contain quantum numbers for the upper and lower states, respectively.

References

Aliev, M. R., & Hougen, J. T. 1984, J. Mol. Spectrosc., 106, 110
Cohen, E. A., & Pickett, H. M. 1982, J. Mol. Spectrosc., 93, 83
De Lucia, F. C., & Helminger, P. 1975, J. Mol. Spectrosc., 54, 200
Di Lonardo, G., & Trombetti, A. 1981, Chem. Phys. Lett., 84, 327
Fusina, L., Di Lonardo, G., & Johns, J. W. C. 1985, J. Mol. Spectrosc., 112, 211
Fusina, L., Di Lonardo, G., Johns, J. W. C., & Halonen, L. 1988, J. Mol. Spectrosc., 127, 240
Fusina, L., & Murzin, S. N. 1994, J. Mol. Spectrosc., 167, 464
Garvey, R. M., De Lucia, F. C., & Cederberg, J. W. 1976, Mol. Phys., 31, 265
Helminger, P., De Lucia, F. C., & Gordy, W. 1971, J. Mol. Spectrosc., 39, 94
Helminger, P., & Gordy, W. 1969, Phys. Rev., 118, 100
Hougen, J. T. 1972, J. Chem. Phys., 57, 4207
Hougen, J. T., & Oka, T. 1981, J. Chem. Phys., 74, 1830
Job, V. A., Kartha, S. B., Singh, K., & Kartha, V. B. 1987, J. Mol. Spectrosc., 126, 290
Kukolich, S. G., & Wofsy, S. C. 1970, J. Chem. Phys., 52, 5477
Lis, D. C., Gerin, M., & Roueff, E. 2005, in The Dusty and Molecular Universe: A Prelude to Herschel and ALMA, 381
Lis, D. C., Gerin, M., Roueff, E., Vastel, C., & Phillips, T. G. 2006, ApJ, in press
Lis, D. C., Roueff, E., Gerin, M., et al. 2002, ApJ, 571, L55
Marshall, M. D., & Muenter, J. S. 1981, J. Mol. Spectrosc., 85, 322
Müller, H. S. P., Thorwirth, S., Roth, D. A., & Winnewisser, G. 2001, A&A, 370, L49
Pagani, L., Lagache, G., Bacmann, A., et al. 2003, A&A, 406, L59
Pagani, L., Bacmann, A., Motte, F., et al. 2004, A&A, 417, 605
Pagani, L., Pardo., J.-R., Apponi, A. J., Bacmann, A., & Cabrit, S. 2005, A&A, 429, 181
Pickett, H. M., Poynter, R. L., Cohen, E. A., et al. 1998, J. Quant. Spectrosc. Radiat. Transfer, 60, 883
Poynter, R. L., & Kakar, R. K. 1975, ApJS, 29, 87
Poynter, R. L., & Margolis, J. S. 1983, Mol. Phys., 48, 401
Roueff, E., Lis, D. C., van der Tak, F. F. S., Gerin, M., & Goldsmith, P. F. 2005, A&A, 438, 585
Roueff, E., Tiné, S., Coudert, L. H., et al. 2000, A&A, 354, L63
Thaddeus, P., Krisher, L. C., & Loubser, J. H. N. 1964, J. Chem. Phys., 40, 257
Tiné, S., Roueff, E., Falgarone, E., Gerin, M., & des Forêts, G. P. 2000, A&A, 356, 1039
Townes, C. H., & Schawlow, A. L. 1955, Microwave Spectroscopy (New York: McGraw-Hill Book Company)
Urban, Š., Papoušek, D., Kauppinen, J., Yamada, K., & Winnewisser, G. 1983, J. Mol. Spectrosc., 101, 1
van der Tak, F. F. S., Schilke, P., Müller, H. S. P., et al. 2002, A&A, 388, L53
van Veldhoven, J., Jongma, R. T., Sartakov, B., Bongers, W. A., & Meijer, G. 2002, Phys. Rev. A, 66, 032501